

Can I see an Example? Active Learning the Long Tail of Attributes and Relations

Tyler L. Hayes^{1*}, Maximilian Nickel², Christopher Kanan^{1,3},
Ludovic Denoyer⁴, and Arthur Szlam²

¹ Rochester Institute of Technology, Rochester NY, USA

² Facebook AI Research, New York NY, USA

³ Cornell Tech, New York NY, USA

⁴ Facebook AI Research, Paris, France

Abstract. There has been significant progress in creating machine learning models that identify objects in scenes along with their associated attributes and relationships; however, there is a large gap between the best models and human capabilities. One of the major reasons for this gap is the difficulty in collecting sufficient amounts of annotated relations and attributes for training these systems. While some attributes and relations are abundant, the distribution in the natural world and existing datasets is long tailed. In this paper, we address this problem by introducing a novel incremental active learning framework that asks for attributes and relations in visual scenes. While conventional active learning methods ask for labels of specific examples, we flip this framing to allow agents to ask for examples from specific categories. Using this framing, we introduce an active sampling method that asks for examples from the tail of the data distribution and show that it outperforms classical active learning methods on Visual Genome.

Keywords: Active Learning, Long-Tailed Data, Scene Graphs

1 Introduction

In this work, we study the problem of learning to predict attributes and relations in scene graphs. Scene graphs are rich representations of images that encode the positions and attributes of objects along with their relationships to each other [46]. In a scene graph, nodes are defined by boxes labeled with the object class, and edges are defined by the relationship/correlation between these objects. While training machine learning models to produce scene graphs has advanced, performance remains far from optimal. A potential reason is that existing datasets are not sufficiently large, especially for the attributes and relationships.

Because acquiring annotations for scene graphs is challenging, active learning could significantly improve the quality of these datasets by intelligently acquiring additional annotations. In conventional active learning, a learning agent is

* Work done while interning at Facebook AI Research

given unlabeled examples and it selects an informative subset to be labeled by an oracle to improve its performance [59,88,104,109,114]. Ideally, this would enable the agent to achieve better performance with less labeled data. In effect, these systems aim to improve average classification accuracy by having a limited budget for asking questions of the form “What is the label of example i ?”

However, we show in our experiments that conventional active learning approaches perform no better than random selection. We hypothesized that this failure is because the set of possible attributes and relations in scene graphs is long-tailed [96], i.e., there are many attribute and relation classes but the number of instances of each class varies tremendously (see Fig. 2). Typically there is greater uncertainty and worse performance for classes with fewer examples than those with many, i.e., performance is better for the “head” classes than the “tail” classes. Unfortunately, our experiments demonstrate that classical active learning methods fail to explore the tail.

Unlike conventional active learning, humans are capable of asking questions far beyond the label of individual examples. Here, we flip the active learning setting and introduce the Query-by-Category (QBCat) active learning framework where the agent asks to see examples of specific class labels (see Fig. 1 and Fig. 3 for an overview). By asking for class labels, instead of examples, an agent can explicitly sample from the tail of the class distribution. By switching the framing to allow the agent to ask for examples of specific attribute or relation classes, we significantly improve results on tail classes compared to conventional active learning, without sacrificing performance on more frequent classes.

We make the following major contributions: We introduce a novel incremental active learning framework, coined “Query-by-Category” (QBCat), that allows agents to ask for labels at the *category* level instead of the *example* level. To demonstrate the effectiveness of our proposed framework, we study active learning on a new problem domain: training agents to predict objects, attributes, and relations in scene graphs. Since the distribution of attributes and relations is naturally long-tailed, we introduce two methods to enable incremental long-tailed learning including class re-balancing and bias correction. These methods enable learners to perform well on both the natural data distribution, as well as the tail of the distribution. Finally, we use our Query-by-Category framework to introduce a new active sampling approach that samples efficiently

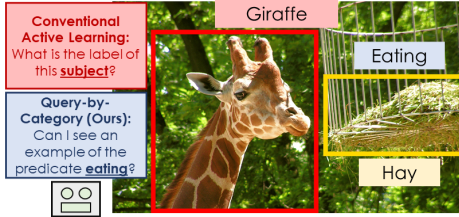


Fig. 1: In conventional active learning, an agent selects unlabeled *examples* that it is most uncertain about to be labeled by an oracle. Conversely, we allow agents to ask for examples at the *category* level instead of the example level. Here, we train agents to predict attributes and relations in scene graphs. Our framing allows the agent to ask for an example of a rare predicate category “eating” and a human annotator provides an example of this predicate.

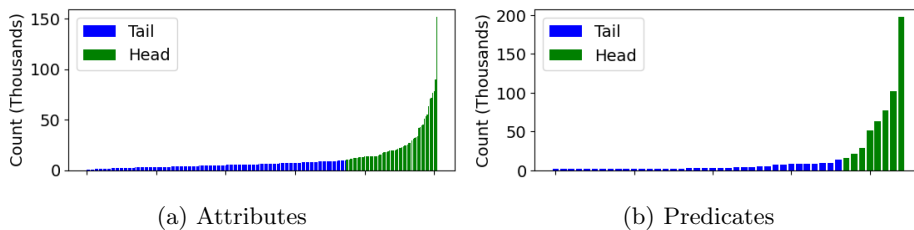


Fig. 2: Histograms of attribute and predicate train distributions. Details about the choice of head and tail classes are in Sec. 5.3.

from the tail of the attribute and relation class distributions. We experimentally validate the effectiveness of class re-balancing and bias correction for long-tailed learning across active learning methods on the Visual Genome dataset [56]. We then demonstrate the effectiveness of our new active sampling method, which outperforms conventional active learning methods on Visual Genome [56].

2 Motivation for Query-by-Category Learning

Suppose we want to use active learning to train an agent. With conventional active learning, the agent needs to compute uncertainty scores over a pool of unlabeled examples to choose examples to be labeled by an oracle. While straightforward, this approach has several drawbacks: a representative set of unlabeled examples must be collected and provided to the learner, the learner must perform inference on all unlabeled examples to compute uncertainty scores, and the model must have a robust estimate of its uncertainty for example selection. Collecting a diverse set of unlabeled examples and performing inference on these examples can be time consuming for annotators and the model, respectively. Moreover, the gamut of possible queries the model can ask about examples is limited, i.e., the model simply asks for the label of an unlabeled example.

We argue that it could be more beneficial to allow a model to ask directly for samples from classes it would like to see, i.e., if the agent knows it is uncertain about the “bicycle” class, then it could ask directly for an example of a “bicycle.” This eliminates the need for model inference on a pool of unlabeled data. Moreover, by asking for classes directly, the agent will likely see a wider variety of classes, which is critical for long-tailed learning. To implement this setup practically, an annotator could be augmented with a search engine or lots of thumbnail images to quickly find images containing a specific class. Alternatively, the learner itself could be provided with a search engine or database to gather labeled data for itself. We leave these implementations for future work; here we are first interested in determining if the Query-by-Category framing yields performance benefits over conventional active learning.

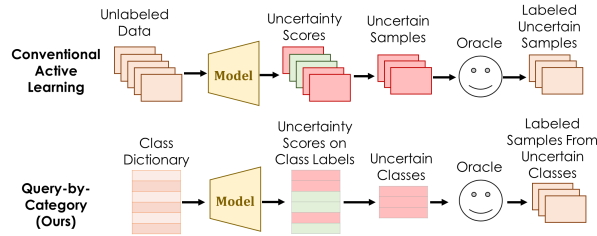


Fig. 3: In conventional active learning, unlabeled data is pushed through a model to obtain uncertainty scores for each example. Uncertain examples are then labeled by an oracle. Conversely, our framework provides a model with a dictionary of classes. The model identifies classes it is uncertain about and queries an oracle for examples from these classes. Unlike conventional methods, our Query-by-Category framework does not require model inference on unlabeled data.

3 Methods

We operate on *scene graphs* [46], consisting of $(subject, predicate, object)$ triples in images. The subject will be a bounding box marking a region of pixels (e.g., an object) in an image. The object might be another bounding box if the predicate is a spatial relationship, like “to the left of”; or a string like “blue” (which could correspond to a predicate like “has color”). If the object is a string, we use the notation $(subject, predicate, attribute)$. We do not consider higher arity relations or relations that cross multiple images.

The learning agent will be tasked with predicting the missing element in an incomplete triple. We denote the triple with two known elements as the *question* and the correct missing element as the *target*. We use s , o , p , and a to denote subjects, objects, predicates, and attributes respectively. This yields six unique question types: $(?, p, o)$ and $(?, p, a)$ where the target is a subject, $(s, ?, o)$, and $(s, ?, a)$ where the target is a predicate, $(s, p, o?)$ where the target is an object, and $(s, p, a?)$ where the target is an attribute.

Rather than assuming the labeled data is fixed at the start of learning, we operate in an incremental active learning setting. Here, the agent can ask for a fixed number of annotations over a sequence of increments. However, we will see that classical active learning techniques do not significantly improve on random selection, in part due to the long tail of attributes and relations. Our main result is that asking for examples of a triple (described in more detail in Sec. 3.3) is more effective at exploring the tail of possibilities than asking for completions of triples. However, this active sampling strategy biases the model to the tail; and reduces performance on the natural distribution. We will see that combined with proper re-biasing techniques (Sec. 3.2), we get the best of both worlds: improved tail performance without sacrificing accuracy on the natural distribution.

3.1 Incremental Training Procedure

Let \mathcal{D}_L and \mathcal{D}_U denote labeled and unlabeled subsets of the dataset $\mathcal{D} = \mathcal{D}_L \cup \mathcal{D}_U$, respectively, where \mathcal{D} is a dataset of triples. The “unlabeled” triples correspond to the “questions” from above; whereas “labeled” examples are the complete triple (question and target together). For the rest of the paper, we will use “natural distribution” to refer to either the base distribution on \mathcal{D} or to targets in \mathcal{D} ; and the “head” to refer to the elements in \mathcal{D} with the most common targets (or to those targets themselves), and the “tail” to refer to other targets (see Fig. 2 for head and tail attribute and predicate distributions).

In the real world, an agent would receive a stream of inputs from its environment for which it could incrementally ask questions to improve its world model. Motivated by this setup, we perform incremental active learning as follows. We first pre-train the model on \mathcal{D}_L drawn from the head of the training data. We wish to simulate the setting where we first collect some seed data (which, following the natural distribution, would mostly come from the head), and then the learning agent actively learns starting from a model pre-trained on the seed data. After pre-training, we initialize an experience replay buffer with all pre-training data. Then, an active sampling strategy (described in Sec. 5.1) is used to select B samples from the unlabeled dataset (\mathcal{D}_U) to be labeled by an oracle.

After the selected samples have been labeled, training is divided into two stages: cross-validation and full model training. Cross-validation is used to determine the number of epochs for full model training to prevent overfitting on a small set of new samples; see Sec. S2.1 for details. After cross-validation, we reset the model parameters to the beginning of the increment, retrain with the validated hyper-parameters, and optionally re-bias to the natural data distribution (see Sec. 3.2). We then evaluate the model (see Sec. 5) and put all newly labeled examples in the replay buffer and repeat. We refer to the process of adding new data, cross-validation, training, and then optional re-biasing as an “increment.”

3.2 Methods to Handle Class Imbalance

Because of the long-tailed data distribution, naive training on increments leads to over-fitting on the head classes; and more generally, hinders learning after the first increment (see Sec. S4.3). To address these challenges, we re-balance mini-batches during increments such that there are equal amounts of old (frequently represented) data and new (possibly less frequently represented) data. See Sec. S2.2 for details. This allows learning past the first increment; but results in the model learning a distribution different from the natural distribution. To address this, we perform a re-calibration/bias correction phase after training the model on new data to adjust its outputs for the natural distribution.

Bias Correction. Since we train the model on mini-batches consisting of equal splits of new and old data, the network learns new data better and more quickly, at the cost of not being properly biased for the natural distribution. One way to

remedy this problem in long-tailed settings is to perform post-hoc bias correction on network outputs [41,69,79,98,100,110,119]. We perform bias correction in two stages. After training has completed, we save a copy of all model parameter weights. We then fine-tune the model for a small fixed number of epochs on all data in the replay buffer using standard mini-batches (i.e., from the natural distribution). After fine-tuning, we perform class-specific bias correction on predicates for $(s, ?, o)$ questions and on attributes for $(s, p, a?)$ questions since these two question types require a class as the answer. Correction is performed on these two question types independently, but in a similar fashion.

Intuitively, the class-specific bias correction stage learns to adjust class-specific distances to the natural distribution. Our formulation is reminiscent of Platt scaling [78], which has been effective for model calibration [33]. Specifically, we compute network predictions for all $(s, ?, o)$ or $(s, p, a?)$ questions. We then compute target embeddings for all predicates or attributes in the class dictionary. We then compute the negative Euclidean distance of each predicted embedding to all target embeddings, which yields a score indicating how likely the predicted embedding is to belong to each class. Finally, we train two parameters per class, α and β , to correct each class score: $s \leftarrow \alpha s + \beta$. These parameters are trained by minimizing a cross-entropy loss between the corrected score and the true label. At the end of these two stages, we evaluate the model and reset the model parameters back to their values from before bias correction. Resetting the parameters allows the model to perform better on balanced distributions and only use bias correction for evaluation in imbalanced settings. We study the impact of re-balancing and bias correction on model performance in Sec. 6.1.

3.3 Query-by-Category Framework

One of the challenges in using conventional active sampling methods is that they rely on the following assumptions: 1) the problem that they are being applied to contains a balanced set of classes, 2) performance is measured using accuracy on the test data, and 3) they ask for the label of a specific example. However, we argue that long-tailed distributions are more common in realistic scenarios and that agents should have the ability to ask more interesting questions beyond asking for just a label. To this end, we propose the Query-by-Category (QBCat) active learning framework that allows a learner to ask for examples from specific classes (see Fig. 3). To query an oracle for P samples, the protocol is as follows: 1) provide a dictionary of attribute and predicate classes to the learner; 2) the learner computes an uncertainty score for each class; 3) the learner uses weighted random sampling with class uncertainty scores as weights to select the class distribution for the P samples; 4) the learner queries an oracle for P samples using the class distribution from 3); and 5) the provided samples are combined with replay data and the model is updated. See Alg. S1 for a detailed overview.

Tail-Based Active Sampling. Using this framework, we propose a simple active sampling method that prioritizes rarely encountered classes. This method assumes that a pre-training phase has occurred on head classes of the dataset.

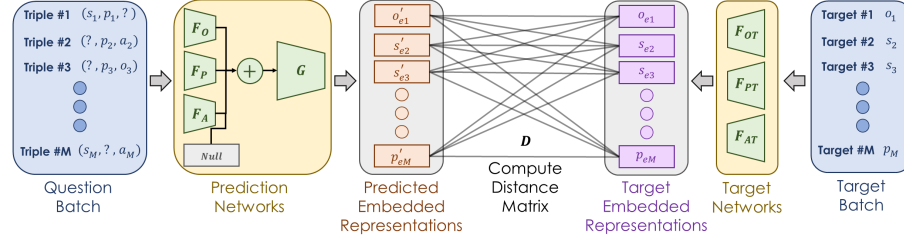


Fig. 4: Our architecture for a mini-batch consisting of M questions (triples) and associated targets. The two elements in the question triple are processed by their respective embedding network (F_O for subjects/objects) or layer (F_P for predicates and F_A for attributes). The resulting embeddings are then concatenated with a trainable Null and processed by the prediction network G , which outputs *predicted* embeddings. Simultaneously, targets are processed by their respective embedding network/layer (F_{OT} for subjects/objects, F_{PT} for predicates, and F_{AT} for attributes) to yield target embeddings. Distances between all pairs of predicted and target embeddings are computed (D) and a categorical cross-entropy loss is computed between D and a target identity matrix via Eq. 1.

During active learning, it assigns class uncertainty scores to tail classes uniformly at random. The oracle then provides the learner samples for the selected classes uniformly at random. While simple, conventional active learning methods often do not consider the label distribution of the data to be learned, which can hinder their performance. We call this method **QBCat-Tail** as it prioritizes learning tail examples.

3.4 Model Architecture

We describe a simple architecture, inspired by [24], which takes an incomplete triple (question) as input and outputs a prediction for the missing element in the triple (see Fig. 4 for an architecture depiction). The basic design is to represent each subject, object, or predicate as a vector. For the subjects and objects that are bounding boxes, we ROI pool features of ground truth boxes from a Faster R-CNN object detection model [81] pre-trained on MS-COCO [58] (see Sec. S2.4). For predicates and objects that are strings, we use a lookup-table embedding.

Each triple contains two known elements and one missing element. The elements are either subject/object vectors $s, o \in \mathbb{R}^{d_o}$, a predicate label $p \in \mathbb{R}$, or an attribute label $a \in \mathbb{R}$. We define a feed-forward neural network $F_O : \mathbb{R}^{d_o} \rightarrow \mathbb{R}^d$, which embeds a subject/object vector in d -dimensional space. Next, we define two embedding layers F_A and F_P to embed an attribute or predicate in d -dimensional space respectively. We then define one trainable $\mathbf{N} \in \mathbb{R}^d$ (for “Null”) per data type to represent the missing element in a triple, i.e., \mathbf{N}_A , \mathbf{N}_P , and \mathbf{N}_O represent a missing attribute, predicate, or subject/object respectively.

During training and evaluation, the two known elements in the triple are embedded in d -dimensional space using the corresponding embedding network/layers, i.e., $h_s = F_O(s)$, $h_o = F_O(o)$, $h_p = F_P(p)$, or $h_a = F_A(a)$. Then, the two embedded representations are concatenated with the appropriate trainable vector \mathbb{N} to yield an embedded vector $h \in \mathbb{R}^{3d}$, where \mathbb{N} is concatenated in the exact location of the missing element in the triple, i.e., the question $q = (s, ?, o)$ maps to $h = [h_s; \mathbb{N}_P; h_o]$. This vector h is processed by another feed-forward network $G : \mathbb{R}^{3d} \rightarrow \mathbb{R}^d$, which outputs the final predicted representation for the missing element in the triple. Similarly, we define a target embedding feed-forward network F_{OT} and two target embedding layers F_{AT} and F_{PT} to embed target subject/objects, attributes, and predicates in d -dimensional space, respectively.

Metric Learning Loss. Given a mini-batch of M questions, a predicted embedding h_q , its associated target embedding t_q , and all pairs between h_u and t_v in the mini-batch, we compute the categorical cross-entropy loss as:

$$\mathcal{L} = -\log \left(\frac{\exp(-\|h_q - t_q\|^2)}{\sum_{u,v} \exp(-\|h_u - t_v\|^2)} \right), \quad (1)$$

which encourages positive pairs to be embedded closer to one another in feature space. This formulation is equivalent to Neighborhood Component Analysis loss [31]. While any distance function could be used, we found Euclidean distance worked best in early experiments, so we use it here.

Model Inference. We evaluate the model in three ways depending on whether the missing element in a triple is a subject/object, a predicate, or an attribute. When the target to be predicted is a subject or object, we first exploit the fact that the answer to the proposed question is limited to subjects and objects in the same scene graph. Thus, we first compute the predicted embedding for the question and then compute target embeddings for each object in the scene graph. We then compute the negative Euclidean distance between the predicted embedding and all possible target embeddings to create a score vector for evaluation. For questions with predicate targets, we compute target embeddings for all possible predicates and a predicted embedding for the question. We then compute the negative distance between the predicted embedding and all target embeddings. The process is identical for questions with attribute targets.

4 Related Work

Scene graphs have been used for many applications (e.g., visual question answering [3,49,67], cross-modal retrieval [105], etc.). Methods have been developed for scene graph classification, detection, generation [99,116,118], and completion [103]. Scene graph completion includes link prediction, which we use here.

Link Prediction on Graphs. In the link prediction task, a neural network is provided with two objects for which it must predict the relationship or “link”

between them. In our setting, a network performs link prediction between objects and node prediction of objects and attributes. Early link predictors were shallow networks that applied simple algebraic operations on node and link embeddings to model relationships [8,60,74,73,95,108,112] (see [72] for a review). Recently, models that use a deep neural network to learn relationships have demonstrated more success due to their expressive power. Knowledge Vault learns to produce outputs when given concatenated subject, relationship, and object embeddings via a multi-layer perceptron network [24]. Lately, Graph Convolutional Networks [22,26,54,86] and Transformers [101] have grown in popularity for processing graph data. Our architecture is inspired by Knowledge Vault, which was chosen due to its simplicity, allowing us to focus on active sampling. Although Knowledge Vault has been applied to textual knowledge graphs, we extend it to visual scene graphs here. Future work could explore alternative architectures.

Long-Tailed Learning. In long-tailed learning, methods tend to overfit to frequently represented classes and not generalize to rarely represented classes. There are three main ways to train with imbalanced data (see [120] for a survey): 1) re-balancing classes (e.g., via re-sampling [14,25,44,66,91], loss adjustment [10,18,53,97], or logit adjustment [41,69,79,100,98,110,119]), 2) transferring information from a pre-training stage or from more to less frequent classes [62,107], or 3) improving model performance via classifier design [50,61,110] or ensembling [34,106,121]. Re-balancing strategies are the simplest to implement and usually achieve comparable performance to more complex methods, so we use them here. Only a few long-tailed active learning approaches have been proposed [2,7,16,32]. Similar to [2], we modify the training setup to make methods more amenable to imbalanced data. Specifically, we re-balance mini-batches with old and new data and bias correct model predictions to the long-tailed distribution. We demonstrate the efficacy of these methods in Sec. 6.1.

Active Learning. Active sampling methods attempt to select the fewest informative examples to be labeled by an oracle [17,59,88,104,109,114]. Active learning strategies fall into three categories: model uncertainty [19,20,21,57,85], diversity-based sampling [32,35,71,87], and expected model change [29,48,90,102]. Uncertainty can be quantified using entropy [40,63,89], discriminator scores [93], the margin between class probabilities [47,82], ensembling [6,30], and model loss [114]. Uncertainty sampling is popular due to its simplicity and ease of use with neural networks, so we use it here. While active learning has been widely explored for classification [6,87,104], detection [27,36,83,94], and semantic segmentation [51,64,92,113], its exploration for node/link prediction has been limited [9,15,65,76]. Most similar to our work are [65,76], which meta-learn an uncertainty-based active sampler. In contrast, we are the first to perform active learning for node/link prediction with a single network on scene graphs. We also propose a new way of performing active learning at the class level.

Incremental Learning. After samples are selected via active learning, a model can be trained from scratch or incrementally fine-tuned on new and old data. Incremental updates are desirable as they are more computationally efficient and can facilitate transfer [5,23,52,77], but are susceptible to catastrophic

forgetting [28,68]. Forgetting can be mitigated using regularization [12,13,55,117], network expansion [38,42,75,84,115], or replay [37,39,43,80,111]. Replay has demonstrated the most success for large-scale problems [11,43,37,80,111], so we use it here. Replay methods maintain old data in a buffer and mix old and new data to update the model. We store all old data in a buffer, which is an upper bound on incremental performance, allowing us to focus on long-tailed active learning. Future work could use buffer management to reduce memory size. Incremental long-tailed learning is relatively unexplored [1,4,44] and has not been applied to visual attribute and relation prediction, so we study it here.

5 Experimental Setup

5.1 Baselines

We perform active sampling on a per question type basis, i.e., we select an equal number of samples from each question type from Sec. 3. We compare four strategies that assign a weight of how likely each unlabeled sample is to be chosen:

Random – This is the simplest approach that uses uniform random weights.

Least Confident – We compute the highest class score for an example. We then invert this score so that examples with the smallest top scores are prioritized.

Minimum Margin – The margin between the highest and second highest score across all class scores for an example is computed [47,82]. We then invert this score to assign higher weights to samples with smaller margins.

Maximum Entropy – An example weight is defined as the entropy of softmaxed scores across classes [63,89,114].

We first assign a weight to each sample in the unlabeled dataset using one of these strategies. We then shift each weight, w_i , such that the smallest weight across samples is 1: $w_i \leftarrow w_i + (1 - \min_j w_j)$. Probabilities are then defined as $p_i = w_i / \sum_j w_j$ and weighted random sampling is used to select samples to be labeled by an oracle. We also compare two baselines. The pre-train baseline is trained on only pre-training data and evaluated immediately after. Pre-train is used to initialize the model for each active learner and is a lower bound. We also train an offline model on all training data, which is an upper bound. Both models are trained with standard mini-batches without bias correction.

5.2 Visual Genome Dataset

We conduct experiments on Visual Genome 1.4 [56], which contains 108,249 images, each with annotated scene graphs. We pre-process the dataset following [45], i.e., we partition the data into train (80%), validation (10%), and test (10%) sets, and filter objects based on size, number of occurrences, and number of associated relationships. This yields 62,565 train, 5,062 validation, and 5,096 test images. The resulting dataset has 253 unique attribute classes (which includes object classes) and 46 unique predicate classes. All (s, p, a) triples use the same predicate (“has attribute”). Given the image dataset with one unique scene

graph per image, we split each relationship edge and each attribute edge into three questions (triples). This yields a dataset with 3,474,969 train, 279,273 validation, and 281,739 test questions. Train and test histograms of attributes and predicates are in Fig. 2 and Fig. S1, respectively.

5.3 Evaluation Protocol and Metrics

We compute performance on the full test set, as well as a test set consisting of only samples from the tail of the attribute and predicate distributions. We define head classes as those containing more samples than the mean across counts over all classes for predicates and attributes separately. This yields 66 head and 187 tail classes for attributes and 9 head and 37 tail classes for predicates. We highlight head and tail classes in the attribute and predicate (minus “has attribute”) distributions in Fig. 2. More details and a list of classes are in Sec. S3.

Given score vectors (from Sec. 3.4) and associated one-hot encodings of the answer, we compute two separate ranking metrics for each of the six unique question types outlined in Sec. 3. Specifically, we compute the area under the receiver operating characteristic (AUROC) curve and the mean average precision (mAP). When a subject or object is the target, we use sample-wise averaging across individual questions since scene graphs do not contain a uniform number of objects, i.e., score vectors are different lengths. When a predicate or attribute is the target, we use micro averaging. While AUROC treats positive and negative classes equally, mAP emphasizes positive classes more than negative ones making it more ideal for long-tailed datasets. In addition to AUROC and mAP, it is also useful to summarize performance over all increments. To do this, we define performance of an offline upper bound as γ_{offline} . Then, given the performance of an incremental learner at increment t as γ_t , we define overall performance as:

$$\Omega = \frac{1}{T} \sum_{t=1}^T [1 - (\gamma_{\text{offline}} - \gamma_t)] , \quad (2)$$

over T increments. If the incremental learner performed as well as the offline method for all increments, then Ω would equal 1. Higher Ω values indicate better performance. Since Ω is normalized to an offline baseline, it is easier to compare Ω scores across question types, metrics, and test sets.

6 Results

Each experiment was conducted with 10 random network initializations and we report the average of each method over all runs. After an initial pre-training phase, all methods performed incremental active learning over 10 increments, where each active sampling method chose 100 samples from each of the six question types at each increment (i.e., 600 selected samples total per increment). Additional implementation details are in Sec. S2, including all training hyperparameters. While $(s, ?, a)$ questions are used during training to provide more

attribute questions, we do not report performance on them since it is uninteresting, i.e., it only requires the model to output that the predicate for an attribute question is “has attribute.” Future work could explore additional predicates for attribute questions such as “has color”, “made of material”, etc. In experiments, our QBCat-Tail method uses the class breakdown from Fig. 2 for determining which classes belong to the tail. Future work could study alternative methods for assigning tail classes (e.g., keeping tally of the number of times each class has been seen by the model).

In Fig. 5, we plot the Ω scores of each method averaged over all five question types on each test set using AUROC and mAP. Raw Ω scores summarizing model performance on each question type are in Table S2. When evaluated on the tail test set, our QBCat-Tail method outperforms baselines by a large margin. For example, in Fig. 5, it outperforms the closest baselines by 6.7% in average Ω AUROC and 3.4% in average Ω mAP. While performance differences are smaller on the full test set, our QBCat-Tail method outperforms the closest baselines by 2.6% and 1.2% in average Ω AUROC and mAP, respectively. The main advantage of our method is its ability to achieve strong performance on tail data without sacrificing performance on head data.

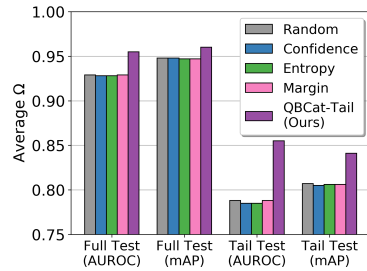


Fig. 5: Average Ω performance of each active learning method over all 10 increments and five question types when evaluated on the full and tail test sets.

To explore performance differences further, we show mAP learning curves for each active learning method in Fig. 6. Learning curves with AUROC and histograms of selected samples are in Sec. S4. Across all increments, our QBCat-Tail method either rivals or outperforms alternative methods across question types and test sets. When evaluated on the full test set, our QBCat-Tail method outperforms all methods by a large margin on box-based questions (i.e., $(?, p, a)$, $(?, p, o)$, and $(s, p, o?)$). For questions where the agent must predict a predicate $(s, ?, o)$ or an attribute $(s, p, a?)$, performance of the QBCat-Tail method on the full dataset is similar to other active learning strategies. QBCat-Tail achieves significant performance improvements across question types on the tail test set.

Across test sets, the $(?, p, a)$ question appears to be the easiest, yielding the highest performance values, while the $(s, ?, o)$ and $(s, p, a?)$ questions are harder, yielding the lowest performance values. This implies that it is easy for models to identify which box contains a specific attribute $(?, p, a)$, but it is more difficult for models to predict a specific attribute given a box $(s, p, a?)$ or a specific predicate given two boxes $(s, ?, o)$. Performance differences among baseline active learners across test sets are minimal, especially in mAP. This is because baseline methods do not explore the tail of the distribution and oversample head data (see histograms in Sec. 6.1). Additional studies of the active learning baselines on only tail data are in Sec. 6.1. One interesting observation is that models recover

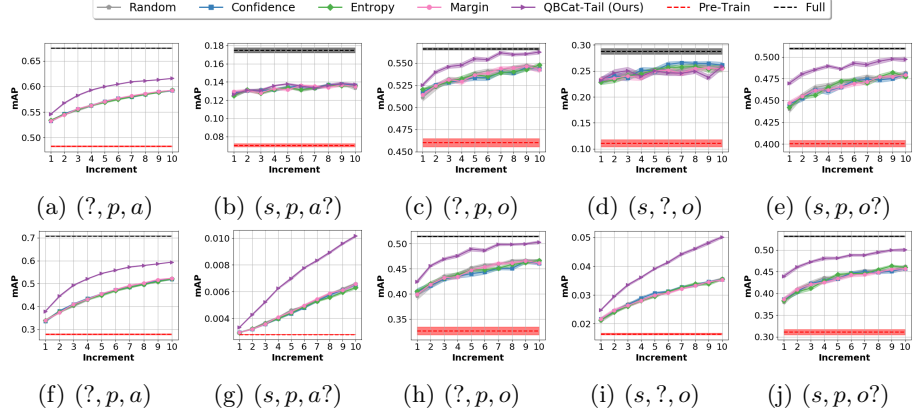


Fig. 6: Learning curves showing incremental learning performance on the **full test set** (top) and **tail test set** (bottom) over 10 increments for each question type. We also include the performance of pre-train (lower bound) and full offline (upper bound) models. Each curve is the average over 10 runs and the standard error over runs is denoted by the shaded region. For plot clarity, the offline upper bound has been removed from the tail plots for $(s, p, a?)$ and $(s, ?, o)$, where the offline baseline achieved an average mAP of 0.312 and 0.263, respectively.

most of the offline performance on the full test set with only 5.5% of the entire labeled dataset. This is desirable as labeled data is costly to obtain.

6.1 Additional Studies

Next, we study several components of our training procedure to identify which yield the most performance improvement. Specifically, we study the average Ω performance of each active learning method in three settings:

Standard Mini-Batches – We train the model using standard mini-batch construction, i.e., batches are sampled uniformly at random without replacement.

Without Bias Correction – We demonstrate model performance when using re-balanced mini-batches without bias correction.

Main Setup – This setup uses re-balanced mini-batches and bias correction.

In Fig. 7, we plot the average Ω AUROC and average Ω mAP scores of each method over all five question types. In supplemental materials, we provide the raw Ω scores for each experiment. On the full test set, we find that performing bias correction is critical to performance across models; however, our QBCat-Tail method is most affected by the absence of bias correction. This is expected as QBCat-Tail prioritizes data from tail classes and its weights must be readjusted for the natural long-tailed distribution via bias correction. On the tail test set, bias correction does not yield any benefit in terms of average Ω mAP, but yields benefit in average Ω AUROC. When evaluating on both the full and tail test

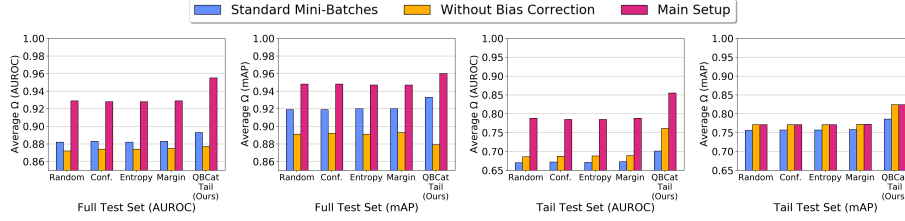


Fig. 7: Average Ω performance of active learners under various setups on the full and tail test sets. Main Setup uses re-balanced mini-batches and bias correction. Each result is averaged over five question types.

sets, using standard mini-batches yields slightly worse performance than using re-balanced batches across methods. It is interesting to note that our QBCat-Tail method outperforms all other methods on both test sets when using standard mini-batches. However, all methods exhibit improved performance when trained using re-balanced mini-batches, motivating their need in long-tailed settings.

Finally, we were interested to see if assigning probabilities to tail samples based on their frequency improved performance of our QBCat-Tail method. In our main experiments, tail classes were selected uniformly at random. We compare this to assigning each tail class a probability equal to $\frac{\text{num_samples_in_class}}{\text{num_samples_in_dataset}}$. Results indicate that frequency-based probabilities yield slightly better performance than uniform probabilities, i.e., the mean performance difference was 0.55% Ω mAP and the maximum performance difference was 1.5% Ω mAP across questions and test sets (see Table S2). Future work could explore more methods for assigning tail probabilities (e.g., class counters, pseudo-labeling).

7 Discussion and Conclusion

We proposed new methods and training paradigms for incremental active learning of long-tailed attributes and relationships. Specifically, we introduced a new Query-by-Category (QBCat) active learning setup which changes the framing of how agents ask an oracle for more training data. It assumes access to a dictionary of class labels and allows models to ask for an example of a particular class instead of following the conventional active learning approach of asking for a label of an uncertain example. We then proposed the QBCat-Tail method and showed that when combined with suitable re-biasing, it performs comparably to existing active learning methods on the natural long-tailed data distribution, and demonstrates significant performance improvements on tail classes. This framing opens the door to several future research directions.

It would be interesting to extend to settings where more than one element in a triple (or a higher order relation) is missing, or to relations spanning multiple images. While we focused on uncertainty-based active learning methods due to

their simplicity, it would also be interesting to explore diversity-based methods that could exploit the metric space learned by our model. We demonstrated that asking for specific classes improved performance over standard active sampling methods. It would be interesting to develop methods that exploit this finding to improve tail performance further. Beyond node/link prediction, our framework could also be extended to full scene graph completion.

Humans and animals interact with their environment to receive supervision to learn and accumulate knowledge. We introduced a new active learning framework and demonstrated its effectiveness on a new problem domain (active learning for scene graph prediction). Further, we introduced a new active sampling method that queries an oracle for examples of a specific class and showed that it outperforms existing baselines. This framing paves the way for future research into how agents should pose questions to an oracle to best improve performance.

Acknowledgements. This work was supported in part by the DARPA/SRI Lifelong Learning Machines program [HR0011-18-C-0051] and NSF award #1909696. The views and conclusions contained herein are those of the authors and should not be interpreted as representing the official policies or endorsements of any sponsor. We thank Robik Shrestha, James Arnold, and Manoj Acharya for their comments and useful discussions.

References

1. Aggarwal, U., Popescu, A., Belouadah, E., Hudelot, C.: A comparative study of calibration methods for imbalanced class incremental learning. *Multimedia Tools and Applications* pp. 1–20 (2021)
2. Aggarwal, U., Popescu, A., Hudelot, C.: Active learning for imbalanced datasets. In: *WACV*. pp. 1428–1437 (2020)
3. Antol, S., Agrawal, A., Lu, J., Mitchell, M., Batra, D., Zitnick, C.L., Parikh, D.: VQA: Visual question answering. In: *ICCV* (2015)
4. Belouadah, E., Popescu, A., Aggarwal, U., Saci, L.: Active class incremental learning for imbalanced datasets. In: *ECCVW*. pp. 146–162. Springer (2020)
5. Belouadah, E., Popescu, A., Kanellos, I.: A comprehensive study of class incremental learning algorithms for visual tasks. *Neural Networks* (2020)
6. Beluch, W.H., Genewein, T., Nürnberger, A., Köhler, J.M.: The power of ensembles for active learning in image classification. In: *CVPR*. pp. 9368–9377 (2018)
7. Bhattacharya, A.R., Liu, J., Chakraborty, S.: A generic active learning framework for class imbalance applications. In: *BMVC*. p. 121 (2019)
8. Bordes, A., Usunier, N., Garcia-Duran, A., Weston, J., Yakhnenko, O.: Translating embeddings for modeling multi-relational data. *NeurIPS* **26** (2013)
9. Cai, H., Zheng, V.W., Chang, K.C.C.: Active learning for graph embedding. *arXiv preprint arXiv:1705.05085* (2017)
10. Cao, K., Wei, C., Gaidon, A., Arechiga, N., Ma, T.: Learning imbalanced datasets with label-distribution-aware margin loss. In: *NeurIPS* (2019)
11. Castro, F.M., Marín-Jiménez, M.J., Guil, N., Schmid, C., Alahari, K.: End-to-end incremental learning. In: *ECCV*. pp. 233–248 (2018)

12. Chaudhry, A., Dokania, P.K., Ajanthan, T., Torr, P.H.: Riemannian walk for incremental learning: Understanding forgetting and intransigence. In: ECCV. pp. 532–547 (2018)
13. Chaudhry, A., Ranzato, M., Rohrbach, M., Elhoseiny, M.: Efficient lifelong learning with A-GEM. In: ICLR (2019)
14. Chawla, N.V., Bowyer, K.W., Hall, L.O., Kegelmeyer, W.P.: Smote: synthetic minority over-sampling technique. *Journal of artificial intelligence research* **16**, 321–357 (2002)
15. Chen, K.J., Han, J., Li, Y.: Hallp: A hybrid active learning approach to link prediction task. *J. Comput.* **9**(3), 551–556 (2014)
16. Choi, J., Yi, K.M., Kim, J., Choo, J., Kim, B., Chang, J., Gwon, Y., Chang, H.J.: Vab-al: Incorporating class imbalance and difficulty with variational bayes for active learning. In: CVPR. pp. 6749–6758 (2021)
17. Cohn, D., Atlas, L., Ladner, R.: Improving generalization with active learning. *Machine learning* **15**(2), 201–221 (1994)
18. Cui, Y., Jia, M., Lin, T.Y., Song, Y., Belongie, S.: Class-balanced loss based on effective number of samples. In: CVPR. pp. 9268–9277 (2019)
19. Culotta, A., McCallum, A.: Reducing labeling effort for structured prediction tasks. In: AAAI. vol. 5, pp. 746–751 (2005)
20. Dagan, I., Engelson, S.P.: Committee-based sampling for training probabilistic classifiers. In: *Machine Learning Proceedings 1995*, pp. 150–157. Elsevier (1995)
21. Dasgupta, S., Hsu, D.: Hierarchical sampling for active learning. In: ICML. pp. 208–215. ACM (2008)
22. Defferrard, M., Bresson, X., Vandergheynst, P.: Convolutional neural networks on graphs with fast localized spectral filtering. *NeurIPS* **29**, 3844–3852 (2016)
23. Delange, M., Aljundi, R., Masana, M., Parisot, S., Jia, X., Leonardis, A., Slabaugh, G., Tuytelaars, T.: A continual learning survey: Defying forgetting in classification tasks. *TPAMI* (2021). <https://doi.org/10.1109/TPAMI.2021.3057446>
24. Dong, X., Gabrilovich, E., Heitz, G., Horn, W., Lao, N., Murphy, K., Strohmman, T., Sun, S., Zhang, W.: Knowledge vault: A web-scale approach to probabilistic knowledge fusion. In: *Proceedings of the 20th ACM SIGKDD international conference on Knowledge discovery and data mining*. pp. 601–610 (2014)
25. Drummond, C.: Class imbalance and cost sensitivity: Why undersampling beats oversampling. In: *ICML-KDD Workshop*. vol. 3 (2003)
26. Duvenaud, D., Maclaurin, D., Aguilera-Iparraguirre, J., Gómez-Bombarelli, R., Hirzel, T., Aspuru-Guzik, A., Adams, R.P.: Convolutional networks on graphs for learning molecular fingerprints. *arXiv preprint arXiv:1509.09292* (2015)
27. Feng, D., Wei, X., Rosenbaum, L., Maki, A., Dietmayer, K.: Deep active learning for efficient training of a lidar 3d object detector. In: *2019 IEEE Intelligent Vehicles Symposium (IV)*. pp. 667–674. IEEE (2019)
28. French, R.M.: Catastrophic forgetting in connectionist networks. *Trends in Cognitive Sciences* **3**(4), 128–135 (1999)
29. Freytag, A., Rodner, E., Denzler, J.: Selecting influential examples: Active learning with expected model output changes. In: ECCV. pp. 562–577. Springer (2014)
30. Gal, Y., Islam, R., Ghahramani, Z.: Deep bayesian active learning with image data. In: ICML. pp. 1183–1192. PMLR (2017)
31. Goldberger, J., Hinton, G.E., Roweis, S., Salakhutdinov, R.R.: Neighbourhood components analysis. *NeurIPS* **17** (2004)

32. Gudovskiy, D., Hodgkinson, A., Yamaguchi, T., Tsukizawa, S.: Deep active learning for biased datasets via fisher kernel self-supervision. In: CVPR. pp. 9041–9049 (2020)
33. Guo, C., Pleiss, G., Sun, Y., Weinberger, K.Q.: On calibration of modern neural networks. In: ICML. pp. 1321–1330 (2017)
34. Guo, H., Wang, S.: Long-tailed multi-label visual recognition by collaborative training on uniform and re-balanced samplings. In: CVPR. pp. 15089–15098 (2021)
35. Guo, Y.: Active instance sampling via matrix partition. In: NeurIPS. pp. 802–810 (2010)
36. Haussmann, E., Fenzi, M., Chitta, K., Ivanecky, J., Xu, H., Roy, D., Mittel, A., Koumchatzky, N., Farabet, C., Alvarez, J.M.: Scalable active learning for object detection. In: 2020 IEEE Intelligent Vehicles Symposium (IV). pp. 1430–1435. IEEE (2020)
37. Hayes, T.L., Kafle, K., Shrestha, R., Acharya, M., Kanan, C.: Remind your neural network to prevent catastrophic forgetting. In: ECCV (2020)
38. Hayes, T.L., Kanan, C.: Lifelong machine learning with deep streaming linear discriminant analysis. In: CVPRW (2020)
39. Hayes, T.L., Krishnan, G.P., Bazhenov, M., Siegelmann, H.T., Sejnowski, T.J., Kanan, C.: Replay in deep learning: Current approaches and missing biological elements. *Neural Computation* **33**(11), 2908–2950 (2021)
40. Holub, A., Perona, P., Burl, M.C.: Entropy-based active learning for object recognition. In: CVPRW. pp. 1–8. IEEE (2008)
41. Hong, Y., Han, S., Choi, K., Seo, S., Kim, B., Chang, B.: Disentangling label distribution for long-tailed visual recognition. In: CVPR. pp. 6626–6636 (2021)
42. Hou, S., Pan, X., Change Loy, C., Wang, Z., Lin, D.: Lifelong learning via progressive distillation and retrospection. In: ECCV. pp. 437–452 (2018)
43. Hou, S., Pan, X., Wang, Z., Change Loy, C., Lin, D.: Learning a unified classifier incrementally via rebalancing. In: CVPR (2019)
44. Hu, X., Jiang, Y., Tang, K., Chen, J., Miao, C., Zhang, H.: Learning to segment the tail. In: CVPR. pp. 14045–14054 (2020)
45. Johnson, J., Gupta, A., Fei-Fei, L.: Image generation from scene graphs. In: CVPR (2018)
46. Johnson, J., Krishna, R., Stark, M., Li, L.J., Shamma, D., Bernstein, M., Fei-Fei, L.: Image retrieval using scene graphs. In: CVPR. pp. 3668–3678 (2015)
47. Joshi, A.J., Porikli, F., Papanikolopoulos, N.: Multi-class active learning for image classification. In: CVPR. pp. 2372–2379. IEEE (2009)
48. Kading, C., Rodner, E., Freytag, A., Denzler, J.: Active and continuous exploration with deep neural networks and expected model output changes. arXiv preprint arXiv:1612.06129 (2016)
49. Kafle, K., Kanan, C.: Visual question answering: Datasets, algorithms, and future challenges. *Computer Vision and Image Understanding* (2017)
50. Kang, B., Xie, S., Rohrbach, M., Yan, Z., Gordo, A., Feng, J., Kalantidis, Y.: Decoupling representation and classifier for long-tailed recognition. *ICLR* (2020)
51. Kasarla, T., Nagendar, G., Hegde, G.M., Balasubramanian, V., Jawahar, C.: Region-based active learning for efficient labeling in semantic segmentation. In: WACV. pp. 1109–1117. IEEE (2019)
52. Kemker, R., McClure, M., Abitino, A., Hayes, T.L., Kanan, C.: Measuring catastrophic forgetting in neural networks. In: AAAI. pp. 3390–3398 (2018)

53. Khan, S.H., Hayat, M., Bennamoun, M., Sohel, F.A., Togneri, R.: Cost-sensitive learning of deep feature representations from imbalanced data. *IEEE transactions on neural networks and learning systems* **29**(8), 3573–3587 (2017)
54. Kipf, T.N., Welling, M.: Semi-supervised classification with graph convolutional networks. *arXiv preprint arXiv:1609.02907* (2016)
55. Kirkpatrick, J., Pascanu, R., Rabinowitz, N., Veness, J., Desjardins, G., Rusu, A.A., Milan, K., Quan, J., Ramalho, T., Grabska-Barwinska, A., Hassabis, D., Clopath, C., Kumaran, D., Hadsell, R.: Overcoming catastrophic forgetting in neural networks. *PNAS* (2017)
56. Krishna, R., Zhu, Y., Groth, O., Johnson, J., Hata, K., Kravitz, J., Chen, S., Kalanditis, Y., Li, L.J., Shamma, D.A., Bernstein, M., Fei-Fei, L.: Visual genome: Connecting language and vision using crowdsourced dense image annotations. *IJCV* **123**(1), 32–73 (2017)
57. Lewis, D.D., Gale, W.A.: A sequential algorithm for training text classifiers. In: *SIGIR'94*. pp. 3–12. Springer (1994)
58. Lin, T.Y., Maire, M., Belongie, S., Hays, J., Perona, P., Ramanan, D., Dollár, P., Zitnick, C.L.: Microsoft coco: Common objects in context. In: *ECCV*. pp. 740–755. Springer (2014)
59. Lin, X., Parikh, D.: Active learning for visual question answering: An empirical study. *arXiv:1711.01732* (2017)
60. Lin, Y., Liu, Z., Sun, M., Liu, Y., Zhu, X.: Learning entity and relation embeddings for knowledge graph completion. In: *AAAI* (2015)
61. Liu, J., Sun, Y., Han, C., Dou, Z., Li, W.: Deep representation learning on long-tailed data: A learnable embedding augmentation perspective. In: *CVPR*. pp. 2970–2979 (2020)
62. Liu, Z., Miao, Z., Zhan, X., Wang, J., Gong, B., Yu, S.X.: Large-scale long-tailed recognition in an open world. In: *CVPR*. pp. 2537–2546 (2019)
63. Luo, W., Schwing, A., Urtasun, R.: Latent structured active learning. *NeurIPS* **26**, 728–736 (2013)
64. Mackowiak, R., Lenz, P., Ghorri, O., Diego, F., Lange, O., Rother, C.: Cereals-cost-effective region-based active learning for semantic segmentation. *arXiv preprint arXiv:1810.09726* (2018)
65. Madhawa, K., Murata, T.: Active learning on graphs via meta learning. In: *ICML Workshop on Graph Representation Learning and Beyond, ICML* (2020)
66. Mahajan, D., Girshick, R., Ramanathan, V., He, K., Paluri, M., Li, Y., Bharambe, A., Van Der Maaten, L.: Exploring the limits of weakly supervised pretraining. In: *ECCV*. pp. 181–196 (2018)
67. Malinowski, M., Fritz, M.: A multi-world approach to question answering about real-world scenes based on uncertain input. In: *NeurIPS* (2014)
68. McCloskey, M., Cohen, N.J.: Catastrophic interference in connectionist networks: The sequential learning problem. *Psychology of Learning and Motivation* **24**, 109–165 (1989)
69. Menon, A.K., Jayasumana, S., Rawat, A.S., Jain, H., Veit, A., Kumar, S.: Long-tail learning via logit adjustment. In: *ICLR* (2021), <https://openreview.net/forum?id=37nvvqkCo5>
70. Misra, D.: Mish: A self regularized non-monotonic neural activation function. In: *BMVC* (2020)
71. Nguyen, H.T., Smeulders, A.: Active learning using pre-clustering. In: *ICML*. p. 79 (2004)
72. Nickel, M., Murphy, K., Tresp, V., Gabrilovich, E.: A review of relational machine learning for knowledge graphs. *Proceedings of the IEEE* **104**(1), 11–33 (2015)

73. Nickel, M., Rosasco, L., Poggio, T.: Holographic embeddings of knowledge graphs. In: AAAI (2016)
74. Nickel, M., Tresp, V., Kriegel, H.P.: A three-way model for collective learning on multi-relational data. In: ICML (2011)
75. Ostapenko, O., Puscas, M., Klein, T., Jähnichen, P., Nabi, M.: Learning to remember: A synaptic plasticity driven framework for continual learning. In: CVPR (2019)
76. Ostapuk, N., Yang, J., Cudré-Mauroux, P.: Activelink: deep active learning for link prediction in knowledge graphs. In: The World Wide Web Conference. pp. 1398–1408 (2019)
77. Parisi, G.I., Kemker, R., Part, J.L., Kanan, C., Wermter, S.: Continual lifelong learning with neural networks: A review. *Neural Networks* (2019)
78. Platt, J.C.: Probabilistic outputs for support vector machines and comparisons to regularized likelihood methods. In: *Advances in Large Margin Classifiers* (1999)
79. Provost, F.: Machine learning from imbalanced data sets 101. In: AAAIW. pp. 1–3. AAAI Press (2000)
80. Rebuffi, S.A., Kolesnikov, A., Sperl, G., Lampert, C.H.: icarl: Incremental classifier and representation learning. In: CVPR (2017)
81. Ren, S., He, K., Girshick, R., Sun, J.: Faster r-cnn: Towards real-time object detection with region proposal networks. In: NeurIPS (2015)
82. Roth, D., Small, K.: Margin-based active learning for structured output spaces. In: ECML. pp. 413–424. Springer (2006)
83. Roy, S., Unmesh, A., Namboodiri, V.P.: Deep active learning for object detection. In: BMVC. vol. 362, p. 91 (2018)
84. Rusu, A.A., Rabinowitz, N.C., Desjardins, G., Soyer, H., Kirkpatrick, J., Kavukcuoglu, K., Pascanu, R., Hadsell, R.: Progressive neural networks. arXiv:1606.04671 (2016)
85. Scheffer, T., Decomain, C., Wrobel, S.: Active hidden markov models for information extraction. In: International Symposium on Intelligent Data Analysis. pp. 309–318. Springer (2001)
86. Schlichtkrull, M., Kipf, T.N., Bloem, P., Van Den Berg, R., Titov, I., Welling, M.: Modeling relational data with graph convolutional networks. In: European semantic web conference. pp. 593–607. Springer (2018)
87. Sener, O., Savarese, S.: Active learning for convolutional neural networks: A core-set approach. In: ICLR (2018), <https://openreview.net/forum?id=H1aIuk-RW>
88. Settles, B.: Active learning literature survey. Tech. rep., University of Wisconsin-Madison Department of Computer Sciences (2009)
89. Settles, B., Craven, M.: An analysis of active learning strategies for sequence labeling tasks. In: EMNLP. pp. 1070–1079 (2008)
90. Settles, B., Craven, M., Ray, S.: Multiple-instance active learning. *NeurIPS* **20**, 1289–1296 (2007)
91. Shen, L., Lin, Z., Huang, Q.: Relay backpropagation for effective learning of deep convolutional neural networks. In: ECCV. pp. 467–482. Springer (2016)
92. Siddiqui, Y., Valentin, J., Nießner, M.: Viewal: Active learning with viewpoint entropy for semantic segmentation. In: CVPR. pp. 9433–9443 (2020)
93. Sinha, S., Ebrahimi, S., Darrell, T.: Variational adversarial active learning. In: ICCV. pp. 5972–5981 (2019)
94. Sivaraman, S., Trivedi, M.M.: Active learning for on-road vehicle detection: A comparative study. *Machine vision and applications* **25**(3), 599–611 (2014)
95. Socher, R., Chen, D., Manning, C.D., Ng, A.: Reasoning with neural tensor networks for knowledge base completion. In: NeurIPS. pp. 926–934 (2013)

96. Steyvers, M., Tenenbaum, J.B.: The large-scale structure of semantic networks: Statistical analyses and a model of semantic growth. *Cognitive science* **29**(1), 41–78 (2005)
97. Tan, J., Wang, C., Li, B., Li, Q., Ouyang, W., Yin, C., Yan, J.: Equalization loss for long-tailed object recognition. In: *CVPR*. pp. 11662–11671 (2020)
98. Tang, K., Huang, J., Zhang, H.: Long-tailed classification by keeping the good and removing the bad momentum causal effect. In: *NeurIPS* (2020)
99. Tang, K., Zhang, H., Wu, B., Luo, W., Liu, W.: Learning to compose dynamic tree structures for visual contexts. In: *CVPR*. pp. 6619–6628 (2019)
100. Tian, J., Liu, Y.C., Glaser, N., Hsu, Y.C., Kira, Z.: Posterior re-calibration for imbalanced datasets. In: *NeurIPS* (2020)
101. Vaswani, A., Shazeer, N., Parmar, N., Uszkoreit, J., Jones, L., Gomez, A.N., Kaiser, L., Polosukhin, I.: Attention is all you need. In: *NeurIPS*. pp. 5998–6008 (2017)
102. Vezhnevets, A., Buhmann, J.M., Ferrari, V.: Active learning for semantic segmentation with expected change. In: *CVPR*. pp. 3162–3169. IEEE (2012)
103. Wan, H., Luo, Y., Peng, B., Zheng, W.S.: Representation learning for scene graph completion via jointly structural and visual embedding. In: *IJCAI*. pp. 949–956. Stockholm, Sweden (2018)
104. Wang, K., Zhang, D., Li, Y., Zhang, R., Lin, L.: Cost-effective active learning for deep image classification. *IEEE Transactions on Circuits and Systems for Video Technology* **27**(12), 2591–2600 (2016)
105. Wang, S., Wang, R., Yao, Z., Shan, S., Chen, X.: Cross-modal scene graph matching for relationship-aware image-text retrieval. In: *WACV*. pp. 1508–1517 (2020)
106. Wang, T., Li, Y., Kang, B., Li, J., Liew, J., Tang, S., Hoi, S., Feng, J.: The devil is in classification: A simple framework for long-tail instance segmentation. In: *ECCV*. pp. 728–744. Springer (2020)
107. Wang, Y., Gan, W., Yang, J., Wu, W., Yan, J.: Dynamic curriculum learning for imbalanced data classification. In: *ICCV*. pp. 5017–5026 (2019)
108. Wang, Z., Zhang, J., Feng, J., Chen, Z.: Knowledge graph embedding by translating on hyperplanes. In: *AAAI* (2014)
109. Wei, K., Iyer, R., Bilmes, J.: Submodularity in data subset selection and active learning. In: *ICML*. pp. 1954–1963 (2015)
110. Wu, T., Liu, Z., Huang, Q., Wang, Y., Lin, D.: Adversarial robustness under long-tailed distribution. In: *CVPR*. pp. 8659–8668 (2021)
111. Wu, Y., Chen, Y., Wang, L., Ye, Y., Liu, Z., Guo, Y., Fu, Y.: Large scale incremental learning. In: *CVPR*. pp. 374–382 (2019)
112. Yang, B., Yih, W.t., He, X., Gao, J., Deng, L.: Embedding entities and relations for learning and inference in knowledge bases. *arXiv preprint arXiv:1412.6575* (2014)
113. Yang, L., Zhang, Y., Chen, J., Zhang, S., Chen, D.Z.: Suggestive annotation: A deep active learning framework for biomedical image segmentation. In: *International conference on medical image computing and computer-assisted intervention*. pp. 399–407. Springer (2017)
114. Yoo, D., So Kweon, I.: Learning loss for active learning. In: *CVPR*. pp. 93–102 (2019)
115. Yoon, J., Yang, E., Lee, J., Hwang, S.J.: Lifelong learning with dynamically expandable networks. In: *ICLR* (2018)
116. Zellers, R., Yatskar, M., Thomson, S., Choi, Y.: Neural motifs: Scene graph parsing with global context. In: *CVPR* (2018)

- 117. Zenke, F., Poole, B., Ganguli, S.: Continual learning through synaptic intelligence. In: ICML. pp. 3987–3995 (2017)
- 118. Zhang, J., Shih, K.J., Elgammal, A., Tao, A., Catanzaro, B.: Graphical contrastive losses for scene graph parsing. In: CVPR. pp. 11535–11543 (2019)
- 119. Zhang, S., Li, Z., Yan, S., He, X., Sun, J.: Distribution alignment: A unified framework for long-tail visual recognition. In: CVPR. pp. 2361–2370 (2021)
- 120. Zhang, Y., Kang, B., Hooi, B., Yan, S., Feng, J.: Deep long-tailed learning: A survey. arXiv preprint arXiv:2110.04596 (2021)
- 121. Zhou, B., Cui, Q., Wei, X.S., Chen, Z.M.: Bbn: Bilateral-branch network with cumulative learning for long-tailed visual recognition. In: CVPR. pp. 9719–9728 (2020)

Supplemental Material

S1 Algorithmic Overview of the Query-by-Category Active Learning Protocol

A high-level overview of the Query-by-Category active learning protocol is in Alg. S1. To query an oracle for P samples, the protocol is as follows: 1) provide a dictionary of attribute and predicate classes to the learner; 2) the learner computes an uncertainty score for each class; 3) the learner uses weighted random sampling with class uncertainty scores as weights to select the class distribution for the P samples; 4) the learner queries an oracle for P samples using the class distribution from 3); and 5) the provided samples are combined with replay data and the model is updated. Note that this setup requires an initial class dictionary to be provided to the agent. This class dictionary could be initialized using an existing dataset and a human annotator could add more classes to the dictionary over time as scene conditions or objects change.

Algorithm S1: Query-by-Category Active Learning Protocol

Data: Dictionary of classes (\mathcal{C}); Dictionary of question types (\mathcal{Q}); Number of active samples to query per increment per question type (P), Replay buffer containing all pre-training data (\mathcal{R})

Result: Updated model

```

while increment do
    Initialize empty dictionary  $\mathcal{U}$  for class uncertainty scores;
    for  $c$  in  $\mathcal{C}$  do
        Compute uncertainty score  $s$  for class  $c$ ;
        Store uncertainty score:  $\mathcal{U}[c] \leftarrow s$ ;
    end
    Initialize empty active learning data buffer  $\mathcal{B}$ ;
    for  $q$  in  $\mathcal{Q}$  do
        Sample  $P$  classes randomly using class uncertainty scores  $\mathcal{U}$  as weights;
        for  $c$  in  $P$  do
            Query oracle for example from class  $c$  of question type  $q$ ;
            Add new example to buffer  $\mathcal{B}$ ;
        end
    end
    Update model with data from  $\mathcal{B}$  and  $\mathcal{R}$ ;
    Add data from  $\mathcal{B}$  to replay buffer  $\mathcal{R}$ ;
end

```

S1.1 QBCat-Tail Active Sampling

Using the Query-by-Category active learning framework, we propose the QBCat-Tail active sampling method that assigns class uncertainty scores to tail classes uniformly at random. In a deployed setting, one way the QBCat-Tail method could identify samples as belonging to tail classes is by keeping a count of how

many times each class in the class dictionary is visited. Those classes which have been rarely visited would be considered tail classes and assigned a uniform random probability of being selected. Those classes which have been frequently visited would be considered head classes and assigned a probability of zero. Note that QBCat-Tail is just one way of assigning class uncertainty scores and alternative ways of assigning scores using the QBCat framework is an area for future work.

S2 Method Details

We include additional details related to our training paradigm, model architecture, and implementation details in the following subsections.

S2.1 Cross Validation

To perform cross-validation, we first use stratified random sampling to split the experience replay buffer and newly labeled samples into k separate folds each, where k is a hyper-parameter. Then, we combine $(k - 1)$ folds from the experience replay buffer and new samples together to form a training set, and use the remaining held-out sets as a validation set. We train the model on the training set and compute validation loss each epoch. Once the validation loss has not improved for a pre-defined number of epochs (patience), we record the epoch where the model achieved the best validation loss and end cross-validation. While cross-validation is traditionally performed in k separate rounds, we found that using a single round of training/validation was sufficient for determining the optimal number of epochs and reduces compute time, so we use this approach.

S2.2 Re-Balanced Mini-Batches

Since our active sampling methods select very few examples to be labeled in each increment, there is a large imbalance between old samples in the experience replay buffer and newly labeled examples. Further, there is a large imbalance between samples from more frequently and less frequently represented classes due to the long-tailed nature of the training data. To deal with these data imbalances, we perform an epoch in the following way. We iterate over newly labeled examples by selecting a fixed number $M/2$ at each iteration to be included in a mini-batch of size M . After we have iterated over all new data, we shuffle the new data and begin another epoch.

Simultaneously we iterate over all data in the experience replay buffer. For each batch selected from the replay buffer, we first perform hard negative mining to determine which pairs of samples are the most difficult in the batch. Given a batch of replay samples, we perform hard negative mining in the following way. We first find all samples in the mini-batch where the correct answer is not in the top- ℓ predictions output by the network and pair the question example with its top predicted incorrect answer. These hard negative pairs are then added to a

buffer of negatives that is updated each iteration. We use a buffer of negatives to keep track of positive/negative pairs that the model struggles with throughout the increment to ensure that the model maintains performance on previous data.

After hard negative mining, we randomly select $M/4$ pairs of negatives from the buffer to be included in the mini-batch with new examples (i.e., $M/2$ total old samples). After we combine the new samples with the negatives, we update the model for a single iteration. Once we have iterated over the entire experience replay buffer, we shuffle the replay buffer data and begin iterating again. We empty the hard negative buffer at the end of each active learning increment. Since our cross-validation procedure faces the same imbalance problem of many old samples to very few new samples, we use this same re-balanced mini-batch selection procedure to form balanced batches during both the training and validation stages of the cross-validation training stage. We compare this re-balanced mini-batch selection process (which presents an equal number of new and old examples to the model in each batch) to standard mini-batch creation, i.e., uniform random sampling over a combination of new and old data, in our experiments (see Fig. 7 and Sec. S4.3).

S2.3 Model Training

Here, we describe the model training procedure from Sec. 3.4 in more detail. Given a mini-batch of M questions and associated targets, we train the model using metric learning. More specifically, for the M questions, we compute the M predicted representations in embedding space and their associated M target representations. We then compute pairwise distances between all combinations of question and target representations using the Euclidean distance metric. That is, we compute a distance matrix $D \in R^{M \times M}$ such that values on the diagonal of the matrix indicate the distance between a predicted embedding representation and the true associated target representation. Values on the off-diagonal indicate distances between unassociated question/target pairs. This formulation allows us to treat distances between true questions and targets as positives during training, while distances between unassociated questions and targets are treated as negatives. Formally, given a mini-batch of M questions and targets, we compute the loss for a positive pair as follows. First, we compute a question embedding h_q and its associated target embedding t_q . Then, given all batch pairs between question embeddings and target embeddings located at indices u and v respectively, we compute a categorical cross-entropy loss for the positive pair as:

$$\mathcal{L} = -\log \left(\frac{\exp(-\|h_q - t_q\|^2)}{\sum_{u,v} \exp(-\|h_u - t_v\|^2)} \right), \quad (\text{S1})$$

which encourages positive pairs to be embedded closer to one another in feature space. This formulation is equivalent to Neighborhood Component Analysis loss [31]. While any distance function could be used, we found Euclidean distance worked best in early experiments, so we use it here.

S2.4 Implementation Details

Our PyTorch code will be released upon acceptance and we include full implementation details next. All feed-forward neural networks in the model architecture use the same network consisting of two layers with 256 units in the first layer and 128 units in the second layer. The first layer is a fully-connected layer with batch norm and a Mish activation function [70], which helps prevent gradient vanishing. The second layer is the same as the first, but replaces the Mish activation with a sigmoid activation such that all output vector entries are between zero and one, which is useful when computing Euclidean distances between vectors.

For cross-validation and full model training, models are trained using stochastic gradient descent with a learning rate of 0.01, a weight decay factor of 10^{-5} , a momentum value of 0.9, and a re-balanced mini-batch size of 512 (i.e., 256 new samples and 256 old samples). Before selecting 256 old samples to be included in the mini-batch, we use a batch size of 800 samples from the replay buffer to perform hard negative mining. For choosing the number of training epochs, we use a cross-validation k value of 5, a cross-validation patience of 10, a validation batch size of 512, and set a maximum limit of 100 epochs. For hard negative mining, we use a top- ℓ value of 3. For the first stage of bias correction, we use the Adam optimizer and train for 10 epochs with a learning rate of 0.01 and cosine annealing. For the second stage of bias correction, we use the LBFGS optimizer and train for 500 iterations with a learning rate of 0.01.

For pre-training models, offline upper bound models, and experiments using standard mini-batches, we use a batch size of 256. We pre-train on 2,500 samples randomly selected from each head predicate class (minus “has attribute”) and head attribute class, which results in 185,000 pre-training samples. We found pre-training for 1 epoch was sufficient for model convergence and using more epochs for pre-training caused overfitting to the head classes. We train the offline upper bounds for 25 epochs.

To encode subjects and objects as vectors, we first pre-train a Faster R-CNN object detection model [81] with a ResNet-50 backbone on the MS COCO dataset [58]. We then use the Faster R-CNN model to extract 1024-dimensional feature vectors after the ROI pooling layer for all ground truth object boxes in all scene graphs. Since we are focused on the node/link prediction task rather than object detection, we assume access to ground truth boxes; however, future work could explore node/link prediction performance when using boxes generated from the region proposal network of the object detection network. We train the Faster R-CNN model from torchvision using the following hyperparameters: backbone=ResNet-50, optimizer=stochastic gradient descent, learning rate=0.02, learning rate decays by a factor of 10 at epochs 16 and 22, momentum=0.9, aspect ratio group factor=3, batch size=2, data augmentation=horizontal flips, epochs=26, weight decay=0.0001, across 8 GPUs. After training, this model achieves an average precision value (at Intersection over Union (IoU) of 0.5) of 50.7% when evaluated on the COCO mini-val set. In all experiments, we assume access to pre-annotated scene graphs from the Vi-

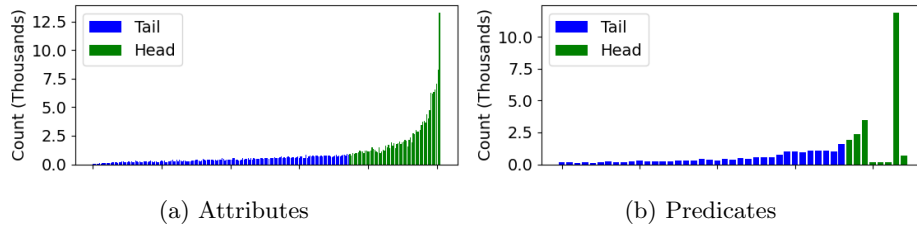


Fig. S1: Histograms of attribute and predicate test distributions.

sual Genome dataset, i.e., we do not use predicted scene graphs from a model. However, using predicted scene graphs could be explored in future work.

S3 Dataset Details

To partition attribute and predicate categories into head and tail classes, we do the following. For attributes, we first compute the number of samples for each class represented in the training dataset. We then compute the mean across counts of all classes, which is equal to 10,973 samples. We then define head attribute classes as those classes containing more than 10,000 samples in the training set and tail attribute classes as those containing fewer than 10,000 samples. Similarly, for predicates, we first compute the number of samples for each class in the training dataset, with the exception of the “has attribute” predicate. The mean across predicate counts is equal to 15,525 samples. Head predicate classes are then defined as those classes containing more than 15,000 samples and tail predicate classes are defined as those classes containing fewer than 15,000 samples. This yields 66 head attribute classes, 187 tail attribute classes, 9 head predicate classes (which includes “has attribute”), and 37 tail predicate classes. Histograms of the counts of all training samples for attribute and predicate classes sorted from smallest to largest are in Fig. 2. The associated histograms containing the counts of all test samples are in Fig. S1. Note that both the train and test distributions are long-tailed. We provide lists of the exact head and tail classes for attributes and predicates below, which are sorted from most to least frequently represented in the training dataset.

Attribute Head Classes:

```
[white, black, tree, man, green, blue, brown, shirt,
 wall, building, window, sky, red, ground, head,
 grass, person, large, woman, hair, table, leg,
 yellow, cloud, sign, gray, car, wooden, pant, grey,
 fence, hand, water, chair, shadow, small, floor,
 tall, door, jacket, leaf, road, line, plate, long,
 field, sidewalk, arm, dark, standing, background,
 people, boy, clear, face, street, snow, metal, ear,
 bush, short, girl, pole, orange, light, bag]
```

Attribute Tail Classes:

[here, tan, track, shoe, jean, glass, bus, picture,
tile, sitting, plant, train, wheel, pillow, branch,
bench, giraffe, rock, silver, tire, umbrella, roof,
tail, pink, wood, dirt, stripe, horse, elephant,
short, flower, big, food, boat, dog, parked, zebra,
coat, hat, bowl, box, hill, mountain, reflection,
neck, brick, wave, cloudy, cabinet, walking, young,
round, striped, bike, house, trunk, open, counter,
helmet, top, cat, handle, mirror, foot, glass,
board, bed, motorcycle, back, clock, ceiling, cow,
bottle, animal, truck, curtain, beach, frame, sand,
banana, shelf, paper, seat, bear, bird, cup, photo,
lady, purple, pizza, ocean, smiling, bare, sheep,
lamp, plastic, windshield, blonde, part, empty, wire,
skateboard, nose, old, child, wing, letter, book,
player, container, looking, wet, railing, kite,
design, plane, stand, basket, sink, edge, wood,
ski, surfboard, bright, towel, brick, cap, logo,
beige, post, writing, finger, vehicle, playing,
concrete, stone, hanging, glove, orange, dirty, calm,
boot, engine, tie, pot, spot, apple, light, little,
colorful, flag, glasses, mouth, grassy, square, dry,
thick, painted, paw, gold, closed, shiny, word,
sock, thin, stone, one, light brown, part, leather,
distant, flying, eye, on, ball, headlight,
rectangular, sticker, number, horn, hole, sunglass,
sliced, button, knob, key, tennis]

Predicate Head Classes:

[has attribute, on, has, in, wearing, of, behind, with,
near]

Predicate Tail Classes:

[next to, on top of, holding, by, under,
in front of, wears, above, sitting on, standing on,
beside, riding, on side of, standing in, over, at,
walking on, attached to, around, hanging on, covering,
below, sitting in, eating, carrying, laying on,
against, have, parked on, for, along, looking at,
belonging to, inside, and, made of, covered in]

Table S1: Accuracy of the Pre-Train and Offline baselines on each question type evaluated on the full and tail test sets. Each result is the average over 10 runs and used to compute the Ω metric.

	AUROC					mAP				
BASELINE	(?, p, a)	(s, p, a?)	(?, p, o)	(s, ?, o)	(s, p, o?)	(?, p, a)	(s, p, a?)	(?, p, o)	(s, ?, o)	(s, p, o?)
<i>Full Test Set</i>										
Pre-Train	0.716	0.769	0.691	0.710	0.663	0.483	0.071	0.460	0.111	0.400
Offline	0.878	0.951	0.794	0.913	0.776	0.675	0.175	0.566	0.288	0.510
<i>Tail Test Set</i>										
Pre-Train	0.515	0.368	0.565	0.402	0.558	0.279	0.003	0.327	0.016	0.311
Offline	0.895	0.960	0.759	0.906	0.783	0.708	0.312	0.515	0.263	0.532

S4 Additional Results

We include a table with baseline model performances as well as raw Ω scores for our main experiments from Sec. 6. We then include learning curves of our main results using the AUROC metric. We then provide tables containing the raw Ω scores for several additional studies involving standard mini-batches, the performance of active learning methods using re-balanced mini-batches without bias correction, and the performance of active learning methods when selecting samples from only tail attribute classes and tail predicate classes. Additionally, we include histogram distributions of the number of samples selected from each attribute class and predicate class by each active learning method.

S4.1 Main Results Tables

Table S1 contains raw accuracies for the Pre-Train and Offline baseline models across question types and test sets. Note that these Offline accuracy values are used for normalization with our Ω metric.

Table S2 contains the raw Ω scores for each active learning method across question types and test sets for our main experiments from Sec. 6. Note that these are the raw Ω scores that are averaged across question types to generate Fig. 5. QBCat-Tail represents the main version of our Tail method that selects classes uniformly at random, while QBCat-Tail (Freq.) represents the additional study of the QBCat-Tail method from Sec. 6.1 that selects classes with probabilities defined by the class frequencies. While the QBCat-Tail (Freq.) method performs the best consistently across metrics, question types, and test sets, QBCat-Tail performs comparably to QBCat-Tail (Freq.) without needing access to class frequencies. QBCat-Tail outperforms or performs comparably to baseline active learning methods when evaluated on the full test set and outperforms baseline methods by a significant margin when evaluated on the tail test set. However, on average, QBCat-Tail outperforms all baseline methods, as shown in Fig. 7.

Table S2: Ω performance of each active learning method over all 10 increments on each question type evaluated on the full and tail test sets. We report performance using both the AUROC and mAP metrics to compute Ω . Each result is the average over 10 runs. QBCat-Tail is our main method that selects classes with uniform random probabilities, while QBCat-Tail (Freq.) selects classes with probabilities defined by the class frequencies. Each method was run using **re-balanced mini-batches and bias correction**.

MODEL	AUROC					mAP				
	(?, p, a)	(s, p, a?)	(?, p, o)	(s, ?, o)	(s, p, o?)	(?, p, a)	(s, p, a?)	(?, p, o)	(s, ?, o)	(s, p, o?)
<i>Full Test Set</i>										
Random	0.917	0.890	0.965	0.915	0.958	0.894	0.958	0.969	0.961	0.959
Confidence	0.918	0.889	0.961	0.917	0.955	0.894	0.959	0.967	0.965	0.957
Entropy	0.917	0.888	0.964	0.915	0.956	0.893	0.957	0.969	0.960	0.957
Margin	0.918	0.890	0.964	0.917	0.956	0.894	0.958	0.969	0.958	0.957
QBCat-Tail	0.941	0.927	0.978	0.951	0.974	0.919	0.959	0.985	0.958	0.979
QBCat-Tail (Freq.)	0.943	0.934	0.983	0.964	0.976	0.921	0.962	0.990	0.973	0.981
<i>Tail Test Set</i>										
Random	0.792	0.581	0.929	0.723	0.915	0.740	0.693	0.931	0.766	0.904
Confidence	0.794	0.576	0.921	0.725	0.910	0.742	0.693	0.925	0.767	0.902
Entropy	0.791	0.574	0.927	0.724	0.911	0.740	0.693	0.928	0.766	0.902
Margin	0.795	0.582	0.927	0.724	0.911	0.743	0.693	0.929	0.766	0.901
QBCat-Tail	0.866	0.695	0.959	0.804	0.951	0.819	0.695	0.965	0.776	0.949
QBCat-Tail (Freq.)	0.872	0.716	0.966	0.836	0.955	0.828	0.696	0.971	0.783	0.954

S4.2 Additional Plots for Main Results

In Fig. 6, we showed learning curves of our main results using the mAP metric. In Fig. S2, we show the same learning curves using the AUROC metric. In AUROC, our tail method outperforms all baselines by a large margin on all question types when evaluated on both the full test set and tail test set. Similar to our results using mAP, baseline active learning methods perform similarly to the random sampling baseline on all question types on both test sets.

Since we perform active sampling at each increment, we also show histograms of the sum of samples selected from different predicate classes and attribute classes by each active learning method after all 10 increments in Fig. S3. Note that we include the main variant of our Tail method that selects classes uniformly (QBCat-Tail), as well as the variant that selects classes based on their frequency (QBCat-Tail (Freq.)). Unsurprisingly, the baseline active sampling methods choose many samples from the head classes, which is likely the reason for their poor generalization to tail classes. Conversely, our tail-based sampling approach only selects samples from the tail of the distribution, allowing it to perform well on a wider variety of classes.

S4.3 Additional Studies with Standard Mini-Batches

In Sec. 3.2, we claimed that naive training using standard mini-batch construction (i.e., uniformly random sampled batches) caused models to overfit to head

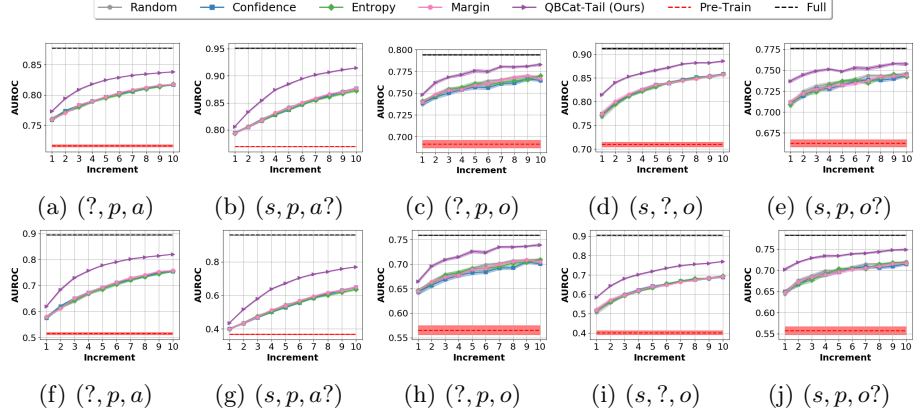


Fig. S2: Learning curves showing incremental learning performance on the **full test set** (top) and **tail test set** (bottom) over 10 increments for each question type. We also include the performance of pre-train (lower bound) and full offline (upper bound) models. Each curve is the average over 10 runs and the standard error over runs is denoted by the shaded region.

classes and impaired learning in later training increments. To support this claim, we compare the mAP performance of the random active sampling baseline using re-balanced mini-batches to using standard mini-batches in Fig. S4. Overall, we see that performance using standard mini-batches is consistently lower than using re-balanced batches, especially when evaluated on the tail test set for $(s, p, a?)$ and $(s, ?, o)$ questions. This motivates the need for re-balanced mini-batches when training on long-tailed data distributions.

Further, we show the Ω performance in AUROC and mAP of each active learning method when using standard mini-batches in Fig. 7 and Table S3. When using standard mini-batches, our QBCat-Tail method still performs comparably to or outperforms baseline active learning methods across question types and test sets. However, performance of all methods is improved by using re-balanced mini-batches, which further motivates their use when operating on imbalanced datasets.

S4.4 Additional Studies Without Bias Correction

While Table S2 contains the results of each active learning method with re-balanced mini-batches after bias correction, we also show the performance of each method without bias correction in Table S4. Recall that the purpose of the bias correction phase is to adjust the network outputs to the natural data distribution. On the full test set, our QBCat-Tail method performs worse than baseline active learning methods for the $(s, p, a?)$ and $(s, ?, o)$ question types. This is not surprising as our method prioritizes selecting tail data and without

Table S3: Ω performance of each active learning method using **standard mini-batches** over all increments when evaluated on the full and tail test sets. We report performance on each question type using both the AUROC and mAP metrics to compute Ω . Each result is the average over 10 runs and computed based on 10 increments.

MODEL	AUROC					mAP				
	$(?, p, a)$	$(s, p, a?)$	$(?, p, o)$	$(s, ?, o)$	$(s, p, o?)$	$(?, p, a)$	$(s, p, a?)$	$(?, p, o)$	$(s, ?, o)$	$(s, p, o?)$
<i>Full Test Set</i>										
Random	0.875	0.834	0.944	0.822	0.936	0.850	0.950	0.949	0.913	0.936
Confidence	0.876	0.835	0.945	0.823	0.936	0.851	0.950	0.948	0.911	0.937
Entropy	0.876	0.834	0.946	0.821	0.934	0.851	0.950	0.950	0.913	0.935
Margin	0.876	0.835	0.948	0.822	0.936	0.851	0.950	0.952	0.911	0.936
QBCat-Tail	0.897	0.834	0.961	0.819	0.955	0.870	0.952	0.968	0.919	0.955
<i>Tail Test Set</i>										
Random	0.663	0.415	0.878	0.534	0.863	0.607	0.691	0.877	0.754	0.851
Confidence	0.668	0.415	0.881	0.535	0.863	0.611	0.691	0.878	0.754	0.853
Entropy	0.666	0.415	0.882	0.531	0.860	0.610	0.691	0.879	0.754	0.850
Margin	0.665	0.415	0.887	0.533	0.863	0.610	0.691	0.886	0.754	0.851
QBCat-Tail	0.730	0.415	0.917	0.537	0.906	0.669	0.691	0.921	0.756	0.894

bias correction, it is not well-calibrated for the natural data distribution. When evaluated on the tail test set, QBCat-Tail outperforms all baselines. However, QBCat-Tail performs comparably to or outperforms other methods on both the full and tail test sets across question types after bias correction is applied in Table S2 and Fig. 7.

S4.5 Active Learning Methods when Selecting Data from Only Tail Classes

Since our QBCat-Tail active sampling method prioritizes data from tail classes during sampling, we were interested to see how other active learning methods performed when selecting data from only tail classes. In this experiment, we compared the random, confidence, entropy, and margin active sampling methods when selecting data from a pool consisting of unlabeled instances from only tail classes (i.e., we removed samples from head classes). Note that random sampling from tail data is equivalent to the QBCat-Tail (Freq.) method from Table S2. Results for each method using Ω when evaluated on the full and tail test sets are in Table S5.

We find that all active sampling methods exhibit performance improvements when selecting samples from only tail data. This further supports the findings of our QBCat-Tail method. While performance is similar for several methods, QBCat-Tail does not require computing uncertainty scores for particular instances, making it simpler and more desirable to use in practice.

It is worth noting that all methods exhibit improved performance on all question types on both test sets when selecting data from only tail classes (compared

Table S4: Ω performance of each active learning method with re-balanced mini-batches **without bias correction** over all increments when evaluated on the full and tail test sets. We report performance on each question type using both the AUROC and mAP metrics to compute Ω . Each result is the average over 10 runs and computed based on 10 increments.

MODEL	AUROC					mAP				
	$(?, p, a)$	$(s, p, a?)$	$(?, p, o)$	$(s, ?, o)$	$(s, p, o?)$	$(?, p, a)$	$(s, p, a?)$	$(?, p, o)$	$(s, ?, o)$	$(s, p, o?)$
<i>Full Test Set</i>										
Random	0.866	0.819	0.937	0.819	0.925	0.830	0.897	0.931	0.872	0.926
Confidence	0.867	0.819	0.936	0.822	0.926	0.831	0.898	0.929	0.877	0.926
Entropy	0.867	0.819	0.938	0.821	0.923	0.831	0.898	0.932	0.869	0.923
Margin	0.866	0.819	0.939	0.822	0.927	0.830	0.898	0.933	0.878	0.927
QBCat-Tail	0.898	0.807	0.944	0.804	0.934	0.864	0.871	0.941	0.780	0.941
<i>Tail Test Set</i>										
Random	0.714	0.419	0.896	0.542	0.860	0.652	0.691	0.898	0.755	0.858
Confidence	0.717	0.419	0.892	0.547	0.862	0.655	0.691	0.894	0.755	0.860
Entropy	0.717	0.419	0.897	0.546	0.860	0.657	0.691	0.897	0.755	0.857
Margin	0.718	0.418	0.899	0.545	0.864	0.656	0.691	0.898	0.755	0.861
QBCat-Tail	0.824	0.443	0.936	0.695	0.908	0.770	0.692	0.948	0.796	0.916

to selecting data from all classes in Table S2), further indicating the benefit of considering the class distribution during active learning on long-tailed datasets. While all methods exhibit improved performance when selecting data from tail classes, our QBCat-Tail approach is simplest since it does not require computing uncertainty scores at the instance level. This motivates the need for more methods that compute uncertainty scores at the class level instead of the instance level.

S4.6 Catastrophic Forgetting and its Relationship to Distribution Mismatch

Incrementally updating neural networks on non-stationary data causes catastrophic forgetting of previous knowledge [28,68]. Catastrophic forgetting is a direct result of the stability-plasticity dilemma; that is, weights of the network must be plastic enough to learn new information, but stable enough to not forget previous information. Here, we argue that the catastrophic forgetting problem is more about domain mismatch than forgetting. For example, we demonstrate that our QBCat-Tail sampling method can maintain performance on old data (frequently represented classes) and new data (possibly less frequently represented classes) by performing a bias correction phase to align the network outputs with the natural data distribution. Even with a bias correction phase to the natural distribution, the network does not catastrophically forget how to classify examples from tail classes. This indicates that with proper distribution alignment techniques, forgetting can become more gradual and less catastrophic.

Table S5: Ω performance of each active learning method when methods **only select data from tail classes** over all increments when evaluated on the full and tail test sets. We report performance on each question type using both the AUROC and mAP metrics to compute Ω . Each result is the average over 10 runs and computed based on 10 increments.

MODEL	AUROC					mAP				
	(?, p, a)	(s, p, a?)	(?, p, o)	(s, ?, o)	(s, p, o?)	(?, p, a)	(s, p, a?)	(?, p, o)	(s, ?, o)	(s, p, o?)
<i>Full Test Set</i>										
Random	0.943	0.934	0.983	0.964	0.976	0.921	0.962	0.990	0.973	0.981
Confidence	0.944	0.933	0.981	0.963	0.974	0.922	0.962	0.986	0.972	0.979
Entropy	0.945	0.934	0.981	0.964	0.974	0.922	0.963	0.987	0.976	0.979
Margin	0.922	0.931	0.972	0.961	0.964	0.897	0.963	0.976	0.971	0.964
QBCat-Tail	0.941	0.927	0.978	0.951	0.974	0.919	0.959	0.985	0.958	0.979
<i>Tail Test Set</i>										
Random	0.872	0.716	0.966	0.836	0.955	0.828	0.696	0.971	0.783	0.954
Confidence	0.876	0.712	0.963	0.834	0.951	0.830	0.696	0.966	0.782	0.949
Entropy	0.877	0.717	0.964	0.836	0.951	0.830	0.696	0.968	0.783	0.949
Margin	0.803	0.708	0.944	0.829	0.927	0.747	0.696	0.944	0.781	0.915
QBCat-Tail	0.866	0.695	0.959	0.804	0.951	0.819	0.695	0.965	0.776	0.949

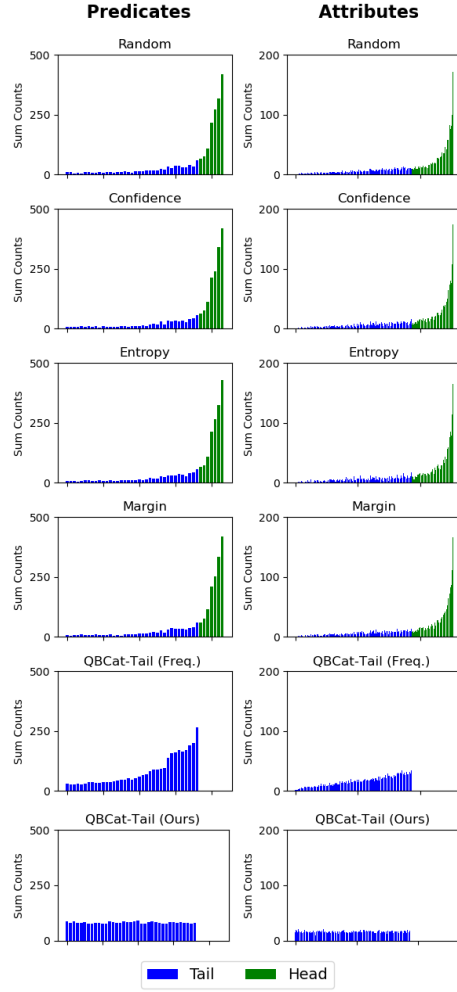


Fig. S3: Sum of counts of each predicate class and attribute class selected during active learning by each method after 10 increments. Each plot is averaged over 10 runs. QBCat-Tail (Ours) is our main method that selects classes with uniform random probabilities, while QBCat-Tail (Freq.) selects classes with probabilities defined by the class frequencies.

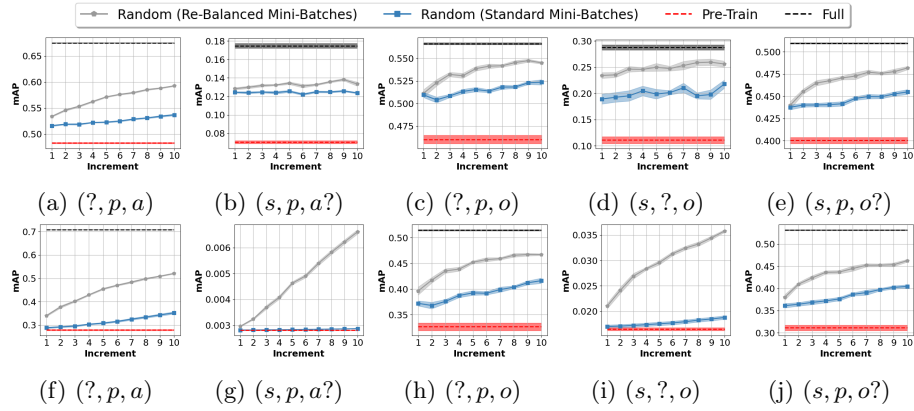


Fig. S4: Learning curves comparing incremental learning performance of the random active sampling method using re-balanced mini-batches and standard mini-batches on the **full test set** (top) and **tail test set** (bottom) over 10 increments for each question type. We also include the performance of pre-train (lower bound) and full offline (upper bound) models. Each curve is the average over 10 runs and the standard error over runs is denoted by the shaded region. For plot clarity, the offline upper bound has been removed from the tail plots for $(s, p, a?)$ and $(s, ?, o)$, where the offline baseline achieved an average mAP of 0.312 and 0.263, respectively.